# Suppression of Edge Localized Modes in High-Confinement KSTAR Plasmas by Nonaxisymmetric Magnetic Perturbations

Y. M. Jeon,[1,*] J.-K. Park,[2] S. W. Yoon,[1] W. H. Ko,[1] S. G. Lee,[1] K. D. Lee,[1] G. S. Yun,[3] Y. U. Nam,[1] W. C. Kim,[1] Jong-Gu Kwak,[1] K. S. Lee,[1] H. K. Kim,[1] and H. L. Yang[1]

(KSTAR team)

[1]*National Fusion Research Institute, Daejeon, Korea*
[2]*Princeton Plasma Physics Laboratory, Princeton, New Jersey, USA*
[3]*Pohang University of Science and Technology, Pohang, Korea*
(Received 5 November 2011; published 20 July 2012)

Edge localized modes (ELMs) in high-confinement mode plasmas were completely suppressed in KSTAR by applying $n = 1$ nonaxisymmetric magnetic perturbations. Initially, the ELMs were intensified with a reduction of frequency, but completely suppressed later. The electron density had an initial 10% decrease followed by a gradual increase as ELMs were suppressed. Interesting phenomena such as a saturated evolution of edge $T_e$ and broadband changes of magnetic fluctuations were observed, suggesting the change of edge transport by the applied magnetic perturbations.

DOI: 10.1103/PhysRevLett.109.035004 PACS numbers: 52.55.Fa, 28.52.−s, 52.35.Py, 52.55.Rk

For a tokamak fusion reactor, the control of edge localized modes (ELMs) in the high-confinement mode ($H$ mode) operation is an essential requirement to avoid excessive heat and particle fluxes onto the plasma facing components (PFCs), which could limit their lifetimes significantly. Among various methods, the application of nonaxisymmetric magnetic perturbations (MPs) has been under very active research in many devices due to its unique feasibility on ELM control. In early years, COMPASS-D tokamak showed that the $n = 1$ MPs ($n$ being the toroidal mode number) could initiate small (type-III) ELMs [1]. Then DIII-D tokamak demonstrated the complete suppression of large (type-I) ELMs for the first time using $n = 3$ MPs by two rows of internal coils [2]. In NSTX tokamak, however, the $n = 3$ MPs for ELM suppression were not successful and instead triggered ELMs on ELM-free plasmas [3]. In the meantime, JET tokamak showed that $n = 1$ MPs by external coils can mitigate the type-I ELMs with increased frequency [4]. Most recently, ASDEX-U tokamak tested the newly installed internal coils and showed successful mitigations of type-I ELMs using the $n = 2$ MPs [5]. In this Letter, we introduce another successful demonstration of ELM control by nonaxisymmetric MPs in KSTAR tokamak, which is uniquely featured by complete ELM suppression using the $n = 1$ MPs with three rows of internal coils.

KSTAR has a versatile in-vessel-control-coil (IVCC) system [6], as shown in Fig. 1(a), which can construct poloidally 3 and toroidally 4 saddle loop connections using field-error-correction (FEC) coils having two turns each. Thus, it can provide toroidal mode variations up to $n = 2$, with various toroidal phase changes among poloidal rows of coils. The three poloidal rows of coils (top-, mid-, and bot-FECs) at the low field side [Fig. 1(b)] were operated by individual dc power converters with maximum currents of 1.9 kA/turn. With $n = 1$ toroidal connection, toroidal phases among three FEC coils can be shifted to 0, ±90, and 180°, from top to bottom, providing different poloidal spectra of perturbed fields. Considering alignment between perturbed field lines to unperturbed plasma field lines, $n = 1$ MP with +90 phase corresponds to the most resonant configuration [Fig. 1(c)] as will be explained later again with Chirikov parameter calculations. Indeed, +90 phased $n = 1$ MP led to the complete ELM suppression whereas other phases did not, indicating the resonant characteristics of ELM-suppressing magnetic perturbations similarly to DIII-D $n = 3$ resonant magnetic perturbations (RMPs).

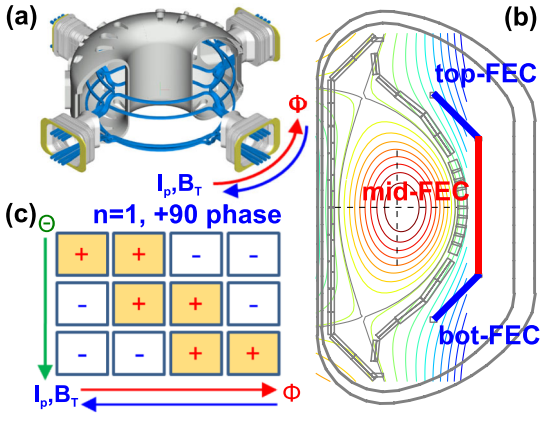


FIG. 1 (color online). (a) KSTAR IVCC coil structure in 3D, (b) the reference equilibrium with three poloidal FEC coils, and (c) the resonant configuration of $n = 1$ MP with +90 phase.

 

A representative ELM-suppressed discharge (#5947) by +90 phased $n = 1$ MP is compared in Fig. 2 with the reference ELMy $H$-mode discharge (#5953). The reference discharge has $I_p = 0.6$ MA with near the double null $D$ shape ($\kappa = 1.9$–$2.0$, $\delta = 0.6$–$0.8$) at $B_T = 2.0$ T, the edge safety factor of $q_{95} = 6$–$7$, and the neoclassical pedestal electron collisionality of $\nu^*_{e,\mathrm{neo}} = 0.5$–$1.0$. The $H$ mode was accessed right after $I_p$ flattop ($\sim 2.0$ sec) with 1.4 MW–90 keV NBI heating and sustained for $\sim 3.0$ sec by preprogrammed plasma control. $D_2$ gas fueling was applied only during the ramp-up phase for $H$-mode access. The confinement enhancement was estimated to $H_{98(y,2)} \sim 0.9$ [7] with rather small ELMs characterized by small drops ($< 1\%$) in density and stored energy at the ELM bursts ($> 70$ Hz). To affect ELM dynamics, the +90 phased $n = 1$ MP with full currents (1.9 kA/turn for each) was applied from 3.0 to 4.5 sec. As shown in $D_\alpha$ signals measured from divertor and midplane regions, initially (3.2–3.7 sec) the spikes from ELM bursts were enlarged with a frequency reduction (ELMs were intensified), and then (3.7–4.3 sec) it disappeared (ELMs were suppressed) until the FEC currents decreased below a certain threshold level. These distinctive two-phase ELM responses also showed different evolutions of various global plasma parameters. The line-averaged electron density was initially dropped by $\sim 10\%$ and then gradually increased in the ELM-suppressed phase. This gradual increase of density ($\sim 0.5 \times 10^{19}$ m$^{-3}$/sec), which is distinguished from a rapid increase of density ($\sim 2.0 \times 10^{19}$ m$^{-3}$/sec) on a natural ELM-free $H$ mode in KSTAR, is a distinctive feature, compared with a controlled density after an initial drop on ELM-suppressed discharges in DIII-D [2]. The stored energy and core rotation velocity were initially dropped by $\sim 10\%$ and then became stationary. Core ion and electron temperatures had relatively small or no changes. Note that there was no change in $D_\alpha$ spike amplitudes observed while the frequency was significantly reduced during the transition from ELM intensification to suppression.

The observations of two distinctive ELM phases, seemingly conflicting each other (intensification vs. suppression), are likely due to mixing of two different magnetic configurations in the applied $n = 1$ MPs. Due to the imperfect FEC control system, there was a time delay of $\sim 0.3$ sec between mid-FEC and other two FEC coils. As shown in Fig. 2(a), the ELM intensification appeared initially when only the mid-FEC current was applied, and then ELMs were suppressed as other two FEC currents were charged up above a threshold value. Therefore, it appears that the main role of mid-FEC alone is intensifying ELMs, while the +90 phased $n = 1$ FEC with all three rows of coils is suppressing ELMs. Indeed, as shown in Fig. 3, a dedicated experiment for the mid-FEC alone showed ELM intensification until the end of the $H$ mode, showing similar parameter evolutions as observed in the initial phase of ELM-suppressed discharges (see Fig. 2). Another important cross-checking will be to charge three rows of coils for +90 phased $n = 1$ FEC simultaneously without a delay and to see if ELMs can be suppressed without initial intensification and degradations of global quantities. In general, it will be necessary to extend experiments and check if the +90 phased $n = 1$ MPs can suppress ELMs fairly independently of ELM characteristics or types. The exact identification of ELM types is another issue to be resolved in the future. Although many evidences, such as ELM energy loss and frequency changes by additional ECH power, imply that the intensified ELMs and even ELMs before MPs are close to type-I, but fairly low $H$-factor [7] and observed precursor oscillations [8]

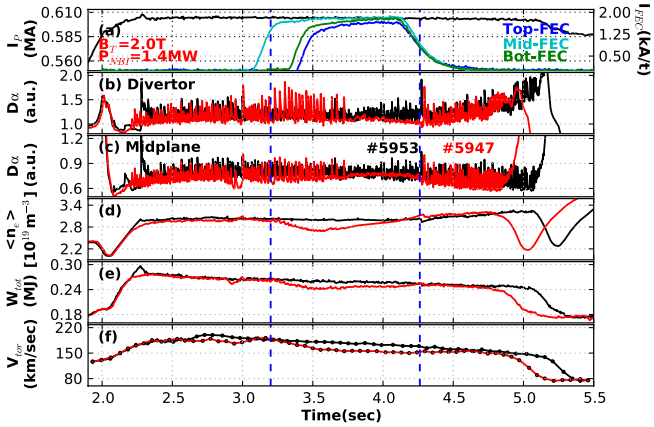


FIG. 2 (color online). An ELM-suppressed discharge (#5947, red) by $n = 1$ (+ 90 phase) MP in comparison with the reference ELMy $H$-mode discharge (#5953, black). (a) Applied FEC currents with $I_p$, $D_\alpha$ signals at (b) divertor and (c) midplane, (d) line-averaged electron density, (e) total stored energy, and (f) toroidal rotation velocity in the core are shown.

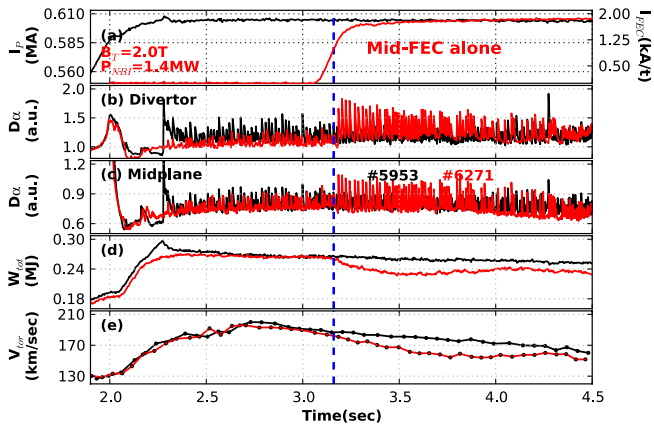


FIG. 3 (color online). An ELM-intensified discharge by $n = 1$ MP with mid-FEC alone in comparison with the reference ELMy discharge. (a) Applied FEC currents with $I_p$, $D_\alpha$ signals at (b) divertor and (c) midplane, (d) total stored energy, and (e) toroidal rotation velocity in the core are shown.

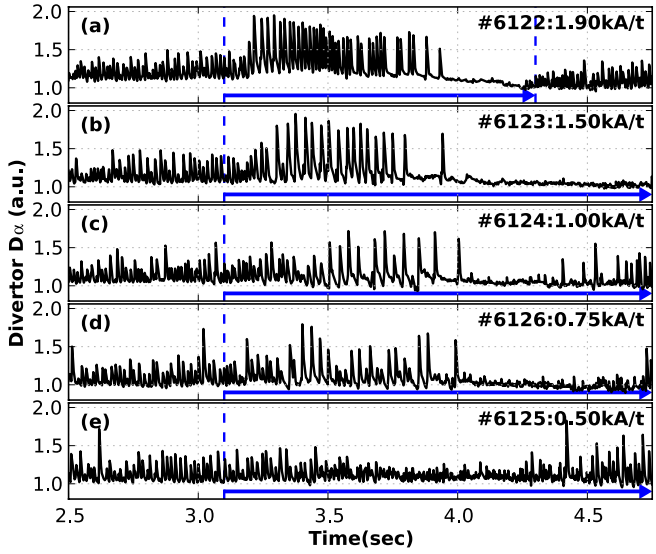


FIG. 4 (color online). ELM responses to different FEC currents (blue arrows) from 0.5 to 1.9 kA/turn, implying that the threshold FEC current for ELM suppression is about 1.5 kA/turn.

before MPs are somewhat unfavorable to this conclusion and should be further clarified.

Another series of experiments were performed with variation of FEC currents from 0.5 to 1.9 kA/turn to investigate the threshold FEC current for ELM mitigation or suppression and also to examine the effect on ELM characteristics. It is found from Fig. 4 that the ELMs can be suppressed fully with FEC currents above 1.5 kA/turn after the initial intensifications. Below that amount ($\geq 0.75$ kA/turn), however, the ELMs were still significantly mitigated (or marginally suppressed) with apparent two-phase ELM responses. It is worth noting that edge safety factors were slowly evolving in these discharges

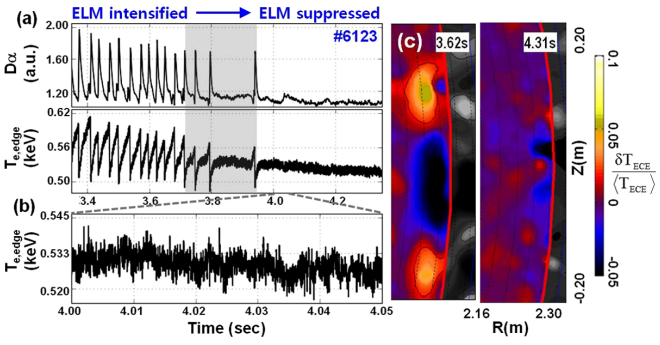


FIG. 5 (color online). (a) Edge ($\rho \sim 0.94$) $T_e$ and $D_\alpha$ evolutions during transition from ELM intensification to suppression. (b) Expanded view of edge $T_e$ on ELM suppression phase. (c) 2D ECE-imaging at the ELM-intensified and suppressed phases. Here, $\rho \sim 0.94$ defined by $\rho \equiv \sqrt{\psi_N}$ with normalized poloidal flux $\psi_N$ is near the top of pedestal. A saturated evolution of $T_e$ pedestal was found during few ELM cycles (gray-shaded period), which was observed up to inside $\rho \sim 0.85$ region.

($\Delta q_{95} \sim 0.5$ based on magnetic EFITs). This indicates that observed ELM alterations by applied $n = 1$ MPs may be not so sensitive to the edge safety factor, although the dedicated experiments with varying $I_P$ or $B_T$ would be required to clarify the issue of the resonant $q$-window.

In principle, the ELM suppression by an application of MPs could have different physics mechanism compared with the ELM mitigation. Therefore it is essential to clarify whether the ELMs were suppressed or significantly mitigated to a very small one. From the edge $T_e$ evolutions measured by electron cyclotron emission (ECE) radiometer with 100 kHz sampling shown in Fig. 5, it can be assessed. Before FEC was on, a typical ELM pattern was observed in edge ($0.85 \sim \rho \sim 0.94$) $T_e$ evolution, reflecting the repetitive forming and crash behaviour of the edge pedestal structure due to ELMs. When the FEC was on [Fig. 5(a)], the patterns were amplified with the increase of period, corresponding to intensified ELMs, and then the repetitive patterns disappeared except some small fluctuating oscillations [Fig. 5(b)] when ELMs were suppressed. The 2D ECE-imaging of the plasma edge [8] for a moment (4.31 sec) in the ELM-suppressed phase also shows no existence of any filamentary structure, while that for a moment (3.62 sec) in the ELM-intensified phase shows poloidally elongated large-size filaments. These observations in ECE and ECE-imaging consistently support the complete suppression of ELMs rather than the mitigation.

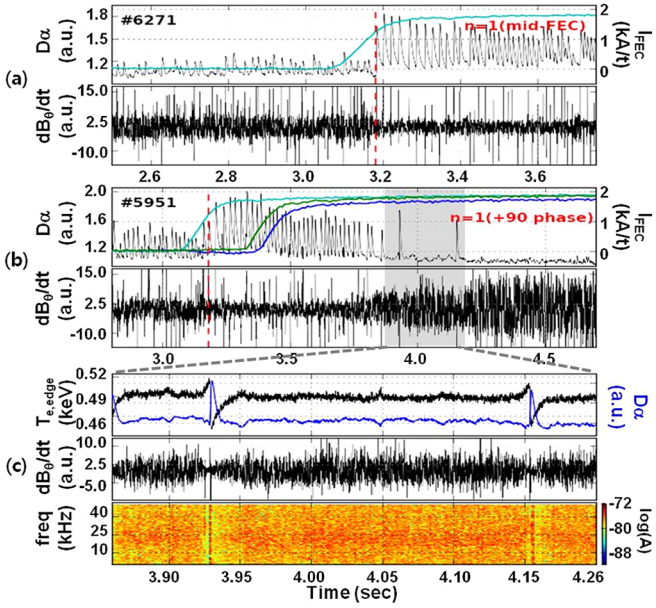


FIG. 6 (color online). Distinctive changes of magnetic fluctuation measured by 100 kHz sampled Mirnov coil signals under different ELM responses. A broadband reduction with ELM-intensification (a) and a broadband increase with ELM suppression (b) are compared together with $D_\alpha$ signals. An expanded view (c) in the transient phase prior to the ELM suppression clearly shows a correlation between the unusual broadband increase of magnetic fluctuation and the saturated evolution of edge $T_e$.

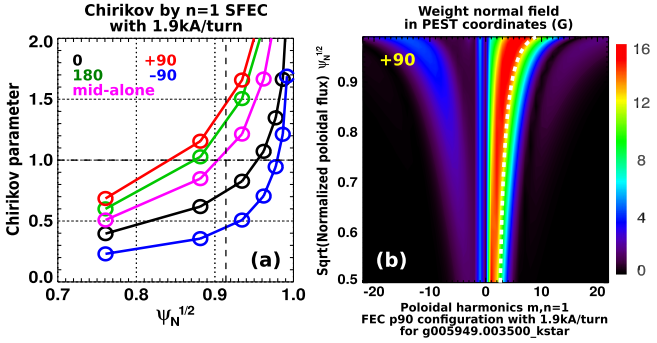


FIG. 7 (color online). (a) Vacuum analysis of Chirikov parameters for various $n = 1$ magnetic spectra. (b) An example of field alignment by vacuum analysis for $n = 1$ with $+90$ phase.

An interesting observation from the edge ($0.85 \sim \rho \sim 0.94$) $T_e$ evolution is that the repetitive patterns were distorted [the grey-shaded period in Fig. 5(a)] during a few cycles prior to the ELM-suppression phase. The monotonic evolution of pedestal forming process was saturated (suggesting enhanced thermal transport) to a certain intermediate level of $T_e$, which corresponds to that in the ELM-suppressed phase. Then when this saturated state became unstable, the monotonic evolution was resumed and continued resulting in an ELM crash. Thus, the ELM suppression, followed by this transient phase, can be characterized by the stably sustained, saturated pedestal evolution. In this regard, it is conjectured that the transport bifurcation from a monotonic evolution to a saturated state may be a key to understand the underlying physics mechanism for the ELM suppression by an application of MP.

Another interesting observation was a broadband change of magnetic fluctuation related to the applied MP spectra and thus ELM responses. It is shown in Fig. 6 that the strength of broadband magnetic fluctuation was reduced with mid-FEC alone resulting in ELM intensification [Fig. 6(a)], while it was gradually increased (dominantly in the midplane) with $+90$ phased $n = 1$ MP resulting in ELM suppression [Fig. 6(b)]. From the expanded view [Fig. 6(c)], it is found that the increase of magnetic fluctuation was correlated with the saturated evolution of edge $T_e$. As shown in the spectrogram, the broadband fluctuation was increased synchronized with the saturated period ($> 90\%$ between the ELM-crashes), while it was reduced just prior to the ELM crashes where the edge $T_e$ resumed a monotonic linear evolution as like in a typical ELM. Note that this broadband activity is distinguished from the coherent modes observed in some natural ELM-free, high-confinement regimes, such as an edge-harmonic-oscillation (EHO) [9] or a weakly coherent mode (WCM) [10].

Although the mechanism of ELM control in application of MPs has not been consistently understood in general, a simple field integration analysis in vacuum can be used to deduce some basic properties of coupling between MPs and plasmas in comparison with different devices. Figure 7 shows the vacuum analysis results for the variation of $n = 1$ magnetic spectra based on the reference equilibrium. According to the estimation of Chirikov parameter [Fig. 7(a)], which becomes the unity ($C = 1$) when adjacent magnetic islands are overlapped, it is expected that the three cases ($+90$, 180, mid-FEC alone) could have thick regions in the edge for overlapped magnetic islands and thus for stochastic magnetic fields, which was believed to be necessary to ELM suppression in DIII-D plasmas. The necessary Chrikov condition, $\psi_N^{1/2} > 0.914$ for $C > 1$ as marked by dotted lines in Fig. 7(a), was determined from large database from DIII-D experiments with ITER-like shape in low collisionality [11]. Also, according to the spectrum analysis of MPs [7(b)], where MPs can be considered resonant if the spectral peak is aligned close enough to the equilibrium field pitch, $q = m/n$ ($n = 1$), as marked by white dot lines in Fig. 7(b), it is expected that the $+90$ phased $n = 1$ is most resonant while the $-90$ phased $n = 1$ is most nonresonant. Therefore, the observed ELM suppression by $+90$ phased $n = 1$ MP is consistent with the vacuum analysis (i.e. importance of resonant condition). However, other results with different magnetic field spectra, such as the ELM intensification by mid-FEC alone and an ELM mitigation by 0 phased $n = 1$ MP (not covered), can not be explained by the vacuum analysis.

In summary, the first ELM suppression by $n = 1$ MPs was successfully demonstrated in KSTAR $H$-mode plasmas showing a two-phase (initially intensified and then suppressed) ELM response related to the mixed magnetic spectra. A gradual increase (after initial 10% drop) of electron density on the ELM-suppressed phase was observed, which is a distinctive feature compared with the controlled density evolution in other devices. Interesting observations are described, which suggest the change of edge transport as the underlying physics mechanism for the ELM suppression by MPs, such as the saturated pedestal evolution on edge $T_e$ and the associated distinctive changes on magnetic fluctuations. Further quantitative studies on edge transport change with application of MPs are planned in the future with improvements of edge diagnostics in KSTAR.

The authors thank Dr. Ahn in Oak Ridge National Laboratory for fruitful discussions. This work was supported by the Korean Ministry of Education, Science and Technology and has been under active collaboration with PPPL.

*ymjeon@nfri.re.kr

[1] S. J. Fielding *et al.*, Europhys. Conf. Abstr. **25A**, 1825 (2001), http://www.cfn.ist.utl.pt/EPS2001/CD/html/pdf/P5.014.pdf.

[2] T. E. Evans *et al.*, Phys. Rev. Lett. **92**, 235003 (2004).

[3] J. M. Canik *et al.*, Phys. Rev. Lett. **104**, 045001 (2010).
[4] Y. Liang *et al.*, Phys. Rev. Lett. **98**, 265004 (2007).
[5] W. Suttrop *et al.*, Phys. Rev. Lett. **106**, 225004 (2011).
[6] H. K. Kim, H. L. Yang, G. H. Kim, Jin-Yong Kim, Hogun Jhang, J. S. Bak, and G. S. Lee, Fusion Eng. Des. **84**, 1029 (2009).
[7] J-W. Ahn *et al.*, Poster (P3.29), *13th International Workshop on H-mode Physics and Transport Barriers, Oxford, UK (2011)* (EFDA-JET, 2011), http://www.jet.efda.org/wp-content/uploads/Ahn.pdf.
[8] G. S. Yun *et al.*, Phys. Plasmas **19**, 056114 (2012).
[9] K. H. Burrell *et al.*, Plasma Phys. Controlled Fusion **44**, A253 (2002).
[10] R. M. McDermott *et al.*, Phys. Plasmas **16**, 056103 (2009).
[11] M. E. Fenstermacher *et al.*, Phys. Plasmas **15**, 056122 (2008).